Published in final edited form as:
J Biomed Mater Res A. 2014 May ; 102(5): 1305–1315. doi:10.1002/jbm.a.34807.

Effects of pore size, implantation time and nano-surface properties on rat skin ingrowth into percutaneous porous titanium implants

Brad J. Farrell[a], **Boris I. Prilutsky**[a], **Jana M. Ritter**[b], **Sean Kelley**[c], **Ketul Popat**[c], and **Mark Pitkin**[d,e]

[a]School of Applied Physiology, Center for Human Movement Studies, Georgia Institute of Technology, Atlanta (GA), USA

[b]St. Joseph's Translational Research Institute, Atlanta (GA), USA

[c]Colorado State University, Fort Collins (CO), USA

[d]Tufts University School of Medicine, Boston (MA), USA

[e]Poly-Orth International, Sharon (MA), USA

Abstract

The main problem of percutaneous osseointegrated implants is poor skin-implant integration, which may cause infection. This study investigated the effects of pore size (Small, 40–100 microns and Large, 100–160 microns), nanotubular surface treatment (Nano), and duration of implantation (3 and 6 weeks) on skin ingrowth into porous titanium. Each implant type was percutaneously inserted in the back of 35 rats randomly assigned to 7 groups. Implant extrusion rate was measured weekly and skin ingrowth into implants was determined histologically after harvesting implants. It was found that all 3 types of implants demonstrated skin tissue ingrowth of over 30% (at week 3) and 50% (at weeks 4–6) of total implant porous area under the skin; longer implantation resulted in greater skin ingrowth ($p<0.05$). Only one case of infection was observed (infection rate 2.9%). Small and Nano groups showed the same implant extrusion rate which was lower than the Large group rate (0.06±0.01 vs. 0.16 ± 0.02 cm/week; $p<0.05$). Ingrowth area was comparable in the Small, Large and Nano implants. However, qualitatively, the Nano implants showed greatest cellular inhabitation within first three weeks. We concluded that percutaneous porous titanium implants allow for skin integration with the potential for a safe seal.

Keywords

Skin-implant integration; porous titanium; nanotubular surface treatment; rat; histology

Corresponding author: Boris I. Prilutsky School of Applied Physiology Georgia Institute of Technology Atlanta, GA 30332-0356, USA Phone: +1-404-894-7659 boris.prilutsky@ap.gatech.edu.

Contribution of authors: BJF and BIP designed the study, performed experiments and wrote manuscript draft, BJF analyzed data and prepared illustrations, MP developed implants, KP and SK developed nanotubular surface treatment, JMR conducted histological analysis, all authors contributed to writing and approved the final manuscript version.

Conflict of interest: No benefit of any kind will be received either directly or indirectly by the authors.

INTRODUCTION

Percutaneous devices allowing access to the body's internal environment for drug delivery, internal monitoring, and external prosthesis attachment have one main problem: the skin-implant interface does not completely isolate the internal environment and permits pathogens to enter the body. At present there is no known artificial material with which skin will readily integrate and effectively seal the exit site of protruding devices. Lack of complete skin integration with the device permits various pathogens to enter the body, which may cause infection[1–3]. Infection can occur in various types of percutaneous devices, including central venous catheters, endotracheal tubes, external fixators and bone-anchored external prostheses. The severity of infection for percutaneous devices depends in part on the amount of infectious agent present at the interface and time since implantation[3,4].

Many biomaterials have been evaluated for skin integration using histological analyses. Previous results on the use of polymers[5–11], tantalum[12,13], titanium[8,14–18], ceramics[19] and other materials have not demonstrated sufficient integration with the skin to prevent bacterial penetration. Of the biomaterials available, titanium has excellent biocompatibility, readily integrates with bony structures and is frequently used in percutaneous applications[8,14–17,20–28].

Titanium implant internal structure and surface treatments may influence skin attachment, ingrowth and overall integration with the implant[29]. Previous research using porous titanium implants has demonstrated the potential for skin cells to distribute throughout the porous titanium and maintain sustainable metabolism inside the implant[15–17,24,30]. Quality of skin integration with porous titanium depends on such factors as pore size, nano scale implant surface topography, and duration of implantation. Porosity influences transportation of nutrients and removal of cellular debris and toxins[1,31]. Nano-textured titanium surface can improve cellular adhesion and increase keratinocyte proliferation and cell spreading compared to machine finished surfaces[32,33]. The decrease in implant surface hardness by the nanotubular surface treatment[34] may also make the nanotube surface layer a promising intermediate structure for the implant-skin interface. Investigations of skin interface with percutaneous porous titanium implants have begun only recently; therefore, there is insufficient information about the effects of the factors discussed above on the quality of skin-implant integration.

The goal of this study was to investigate the effects of pore size, nanotubular surface treatment and duration of implantation on skin ingrowth into porous titanium. We hypothesized that (1) implants with larger pores (100 – 160 μm) would demonstrate more skin ingrowth compared to implants with smaller pores (40–100 μm), (2) nanotubular treatment would increase ingrowth over non-treated implants and (3) a longer period of implantation would result in greater skin ingrowth. Preliminary results of this study have been published in abstract form[35].

MATERIALS AND METHODS

Implants

Porous titanium rods used in the experiments were developed by Poly-Orth International, Sharon, MA, with the manufacturing process for the skin and bone integrated pylon (SBIP-2) being described in detail elsewhere[17,18,36]. The rods (0.3 cm diameter × 2 cm length) with and without nanotubular surface modifications are shown in Fig. 1 A–D. The cylindrical rods were sintered (ADMA Products Group, Hudson, OH) in boron nitride molds (Payne Engineering & Fab. Co., Canton, MA) with Ti6–AL–4V ELI powders provided by ADMA. Three thin (0.5-mm diameter) titanium wires Ti6–AL–4V ELI (Small-Parts,

Seattle, WA) were inserted inside the molds before the 4-hour sintering cycle performed in a Vacuum Industries Super VII furnace (Centorr Vacuum Industries Inc; Nashua, NH, USA) under vacuum $3.333 \cdot 10^{-3}$ Pa. The high temperature sintering was conducted in a vacuum using powders sieved to (−80+200) mesh. Samples were sintered for 4 hours at 1090° C, which was above the beta transus temperature of 996° C. Figure 1A demonstrates a porous titanium rod used in the study and a diagram of a rod cross-section with 3 thin titanium wires. The sintered rods were examined for desired pore size using a scanning electron microscope. The rods of two pore sizes were selected for the study: Small, 40–100 μm, and Large, 100–160 μm, with porosity 45±5%[17,18].

Nanotubular surface treatment was performed on a select group small pore implants at the Colorado State University, Fort Collins, CO (Fig. 1 C–D). Titania nanotube arrays were fabricated using a simple anodization process[37]. Titanium rods were cleaned with soap, acetone and isopropanol, prior to anodization. A two-electrode cell was assembled with titanium foil as the anode and platinum foil as the cathode. The anode-cathode system was introduced into an electrolyte solution, prepared with diethylene glycol (DEG, 99.7%), 2% hydrofluoric acid (HF, 48% solution) and 3% de-ionized water. All treatments were carried out at 60 V for 24 hours at room temperature. Following anodization, the titania nanotube arrays were rinsed with isopropanol and dried with nitrogen gas. Crystallized substrates were obtained by annealing the anodized titania nanotube arrays at 530° C in an oxygen ambient environment for 3 hours. The nanotube architecture was identified using a field emission scanning electron microscope (SEM, JEOL JSM-6300). The substrates were coated with a 10 nm layer of gold prior to imaging at 15 kV. The fabricated nanotubular surfaces had pore diameters ranging from 50 to 250 nm. Mechanical tests revealed the hardness of the nanotube layer to be in the range of 1.5–2.0 GPa compared to 2.0–2.5 GPa for solid titanium. Several 0.3 cm diameter × 2.5 cm length solid titanium implants were used for comparison.

Animals and study design

Two groups of adult rats (at least 6 weeks old, (mass 210–519 g) were used for implantations of porous implants: 25 CD Hairless rats and 10 Sprague Dawley (SD) rats (Charles River, Wilmington, MA, USA). The two different rat species were used in the study to investigate the effects of haired and hairless skin on skin-implant integration. The CD Hairless rats were randomly assigned into groups corresponding to 3 types of implanted pylons (Small, implanted with small pore pylons; Large, implanted with larger pore pylons; and Nano, implanted with small pore pylons with nanotubular surface treatment) and 2 periods of implantation (3 or 6 weeks). The Sprague Dawley rats were randomly assigned into 2 groups: Small and Nano; these groups of rats were implanted for 6 weeks. Five Sprague Dawley rats were also implanted with solid titanium implants as a control group, as solid implants are currently used for attachment of osseointegrated prostheses[23]. Table 1 summarizes study design. All animal procedures were performed in accordance with the US Public Health Service Policy on Humane Care and Use of Laboratory Animals (NIH Publication #85–23 Rev. 1985) and approved by the Institutional Animal Care and Use Committee of Georgia Institute of Technology.

Implantation surgery

Implants were thoroughly washed and autoclaved prior to surgery. Rats were sedated and maintained throughout surgery using isoflurane, 1–3%. The surgical skin area was shaved and scrubbed 3 times with chlorhexidine followed by gauze soaked in isopropyl alcohol. After preparation of the surgical area, the rat was moved to a heated surgical table and covered with a sterile drape with an opening over the area of device implantation on the rat back. The skin between the scapulae was punctured using an appropriate sized biopsy

punch. A sterile implant was then inserted into the skin opening parallel to skin surface leaving approximately 3–5 mm of implant exposed (Fig. 1 E). The initial exposed length was measured using calipers. The implant in skin opening was then secured with several drops of 3M Vetbond tissue adhesive (n-butyl cyanoacrylate; 3M, St. Paul, MN, USA). After allowing time for the adhesive to set, a sterile piece of gauze was placed over the implant for bandaging. The bandage consisted of a single layer of 2.54 cm wide elastic tape (Elastikon, Johnson & Johnson, New Brunswick, NJ, USA) wrapped in an "X" pattern around the forelimbs and chest, as shown in Fig. 1F, followed by a reinforcing strip of cloth-backed tape (Polyken, Evansville, IN, USA). The rats received one injection of anti-inflammatory medication (ketoprofen, 5 mg/kg, SQ) immediately after recovery from anesthesia. The rats were then moved to a separate warm cage for recovery and monitoring and maintained in a 12/12 light/dark cycle with *ad libitum* access to food and water. Bandages were changed at least weekly during measurements of external implant length and rat mass while the animal was anaesthetized with isoflurane, 1–3%. The criteria for terminating the experiment were either the animal reaching the specified implantation time (i.e., 3 or 6 weeks, Table 1) or exposed implant length exceeding 1.5 cm, which corresponded to less than 5 mm of implant remaining beneath the skin. At the terminal experiment, rats were euthanized by carbon dioxide asphyxiation and the implant with skin surrounding the skin-implant interface (at least 1-cm in diameter) was carefully harvested with a sharp scalpel. The implant with skin was placed in 10% neutral buffered formalin for subsequent histological processing and analysis.

Histological and image analyses

After fixation in formalin, samples were infiltrated and embedded in methylmethacrylate blocks, sectioned along the long axis of implant as shown in Fig. 2A using the Exakt System (EXAKT Technologies, Inc., Oklahoma City, OK), and polished. Sections were stained with either haematoxylin and eosin or haematoxylin and basic fuchsin. The entire slide was scanned at high resolution (40x magnification) for image analysis (Nanozoomer, Hamamatsu Corporation, Japan).

Skin ingrowth area and fraction of implant pores filled with skin tissue were determined using a custom Matlab (MathWorks, Natick, MA, USA) program. The region of interest (e.g., the subdermal implant from the outer edge of the epidermis to the deepest portion of the implant, Fig. 2B) was extracted from the larger scanned image at full resolution. The gross edges of the implant were identified. The line separating the internal and external portions of the implant was determined using the outer edges of the epidermis as reference (Fig. 2B, area marked by yellow line). The tissue, implant metal and empty pore areas in the image were determined via brightness thresholds. The threshold values were determined using the program ImageJ[38] based on visual inspection of regions from several different implants. Pixels were identified as implant metal if all the red, green, and blue (RGB) values of the RGB color model were less than 30/255 (< 12%). The image was then converted to hue, saturation, and value (HSV) components to identify the tissue regions (Fig. 2C). Pixels were determined to be tissue if: hue, H > 190/255 (75%); saturation, S > 28/255 (11%); and value, V > 70/255 (27%). The remaining areas of the image were set to be empty space. Using the identified threshold values, a custom image analysis algorithm was written to process the image in blocks of 1000×1000 pixels. The image was then binned into regions for each 10% of the implant subdermal length and width (Fig. 2D) by creating an appropriately sized rectangle to fill the region. The calculated metrics of skin-implant integration included: total area of subdermal implant, metal area, area of empty pores, area of pores filled with skin tissue, and the percentage of pore area filled with skin tissue. The latter was determined as: $Pore\ Fill\ [\%] = 100 \cdot Tissue\ Area\ /(Tissue\ Area + Empty\ Area)$. If

an image bin contained only implant metal (e.g., if the bin covered only a reinforcing wire), that bin was excluded from the analysis.

Statistical analysis

Statistical analysis was performed using STATISTICA 7.0 (StatSoft, Inc., Tulsa, OK). The effect of implant types on the mean implant extrusion length and rate (the slope of the linear regression between the extrusion length and implantation time) was determined using a regression model analysis. The effects of implant type and time duration after implantation on the fraction of pores filled with skin (Fig. 2C) were determined using a two-way ANOVA (Implant: 3 levels and Duration: 2 levels) with Tukey post-hoc tests if significant effects were found. Duration level 1 corresponded to 3 weeks of implantation; duration level 2, 4–6 weeks. The effect of skin hair (or rat species: CD Hairless rats vs. Sprague Dawley (SD) haired rats) on extrusion length and rate and on skin ingrowth was tested using Student's t-tests for independent variables. For all analyses significance level was set to $p < 0.05$.

RESULTS

Total number of implants remaining in the skin through each week of the study is shown in Table 2. Several implants were removed before the set time points because the extruded length reached the endpoint criterion. Depending on removal time, implants were included either in the 3 week implantation group or in the group of longer implantation durations (4–6 weeks). A single solid implant remained implanted for 3 weeks (Fig. 3 B); the other solid implants were either extruded by skin or removed by the rat. Only 1 of the 35 rats implanted with porous implants (2.9%) had to be removed from the study due to clinical signs of infection (i.e., swelling, erythema and pus)[39]. This rat was implanted with a small pore size implant and was removed from the study at 4.5 weeks; initial signs of infection were first noted at 2 weeks (the cause of infection is unknown).

Qualitative analysis

In general the cutaneous tissue was in close apposition to the implant along its length. There was some degree of epidermal downgrowth along the implant surface, which tended to form a pocket with cellular debris between the implant and the skin at the epidermal-implant interface. This epidermal downgrowth stopped a few millimeters below the level of the natural epidermal surface. A serocellular crust composed of degenerate neutrophils and inflammatory debris was present at the exit point of implant from skin, and extended along the exposed surface of the implant (Fig. 3). In many instances, bacterial cocci were present in the crust and sometimes extended into the subjacent peripheral pores of the exposed portion of the implant (Fig. 4 A). However bacteria were not observed in pores of the intradermal portions of implants, except in one rat in which there were clinical signs of infection (see Discussion). Bacterial cultures were taken from the exterior surface of the skin surrounding 4 implants at the time of tissue harvest. The cultures grew *Staphylococcus spp*. of varying antibiotic resistance, consistent with normal skin flora.

All porous implants, regardless of pore size or surface modification, demonstrated signs of tissue ingrowth into the implant pores (Fig. 3 A, C–H). Tissue ingrowth was characterized by filling of pores with fine fibrovascular tissue that extended deep into the implant. Small caliber vessels were recognizable within this tissue in only a few of the small pore implants, but were more pronounced in the large pore implants with implantation times over 4 weeks (Fig. 4 B). The implants with nanotubular surface had more consistent (5/5), diffuse fibrovascular ingrowth into the pores of the embedded portion of the device (Fig. 4C), while

2/5 devices without nano-surface treatment showed more patchy fibrovascular ingrowth accompanied by more significant inflammation (Fig. 4D).

Formation of a fibrous capsule surrounding the intradermal part of the implant was seen (Fig. 3 A,B); it was comprised of connective tissue, small vessels and fibroblasts. Inflammation was sometimes present between the capsule and the implant; when present, inflammation frequently extended into the pores of the implant (Fig 4E).

Quantitative analysis

Implant extrusion length and rate—Implant extrusion lengths for porous Small, Large, and Nano implant groups and the linear regression lines with 95%-confidence limits are shown in Fig. 5A. Extrusion lengths of Solid implants over the course of 3 weeks are also shown for comparison. The slope coefficients of the regression lines (i.e., the rate of extrusion) were positive for all groups of implants ($p<0.05$; Table 3) – the extrusion rate was largest for Solid implants ($p<0.05$), the rate for Large implants was greater than that of Small and Nano implants ($p<0.05$), and there was no significant difference in extrusion rate between Small and Nano implants (Table 3, Fig. 5A). At week 1 of implantation, the mean extrusion length of Solid implants predicted by linear regression (0.42 cm) was significantly greater than that of the Small, Large and Nano implants (0.09–0.16 cm; $p<0.05$). At week 2, the mean extrusion length of Large implants (0.32 cm) became statistically greater than that of Small and Nano implants (0.16–0.23 cm). There was no significant difference in extrusion length between Small and Nano implants throughout 6 weeks of implantation.

Percentage of implant pore area filled with skin tissue—The percentage of pore area filled with skin tissue for different implants and duration of implantation is shown in Fig. 5B. Statistical analysis revealed that implantation time was a significant factor for pore fill percentage; in all types of implants, the area filled with skin tissue was significantly greater for implantations of 4–6 weeks than for implantations of 3 weeks ($F_{1,29} = 23.9$, $p<0.05$). There was no significant difference in percentage of filled pore area between implant types ($F_{2,29} = 0.886$, $p=0.423$). In all types of pylons implanted for up to 3 weeks, at least 30% of pore area was filled with skin tissue; implantation for 4–6 weeks resulted in over 50% of pore area filled.

Distribution of skin ingrowth within implant—The distribution of mean skin tissue ingrowth inside porous implants of different types and implant durations is presented in Fig. 6A. The top row of bins in each panel represents pore area at the upper edge of implant right under the dermis. The left most column represents the bins that would line along the implant exit site; * indicates $bin_{1,1}$ (see Fig 2D diagram for further details). Qualitatively, more skin ingrowth can be seen at the implant end opposite to the exit site irrespective of duration of implantation (Fig. 6A, B). On average, implantation for 4–6 weeks resulted in a greater percentage of skin ingrowth compared to 0–3 week implantations in all types of implants. Statistical analysis showed that implantation time was the only significant factor affecting skin ingrowth and there was no significant effect of implant type (see Fig. 5B and Fig. 6B).

Short term (3 weeks) skin ingrowth outcomes were most favorable for implants with a nanotubular surface (Nano), for which the mean percentage of targeted implant area filled with tissue was highest among the three implant types (Table 4). However, with the low group sample sizes and large standard deviations, there was insufficient power to detect significant difference between group means.

Influence of haired skin on extrusion length and skin ingrowth

The effect of haired skin (or rat species: CD Hairless rats vs. Sprague Dawley (SD) haired rats) was examined by comparing extrusion rate (extrusion rate / implantation time) and skin ingrowth of the 5 CD rats with 5 SD rats implanted with small pore size implants for 6 weeks (Table 1). Extrusion length and rate tended to be higher in CD hairless rats (mean ± SD: 0.43 ± 0.30 cm and 0.08 ± 0.05 cm/week, respectively) compared to SD rats (0.26 ± 0.11 cm and 0.04 ± 0.02 cm/week, respectively), but showed no significant differences ($p > 0.05$, Student's t-test). Skin ingrowth tended to be higher for SD than for CD rats (53.4 ± 13.2 % vs. 41.8 ± 6.0 %), but this difference was not significant ($p > 0.05$, Student's t-test).

DISCUSSION

Hypotheses of the study

The goal of this study was to investigate the effects of pore size, nanotubular surface treatment and duration of implantation on skin ingrowth into porous titanium. It was found that all three types of porous titanium pylons demonstrated skin tissue ingrowth at both 3 weeks and 4–6 weeks of implantation. Pylons with small pore size (40–100 μm) showed fewer signs of extrusion compared to implants with larger pores (100–160 μm), which was in apparent contradiction to our hypothesis 1 that larger pores would demonstrate better skin ingrowth.

Neither pore size nor implant nanotubular surface treatment significantly affected the area of skin ingrowth; thus, hypotheses 1 and 2 were not supported statistically. However, qualitatively, the implants with nanotubular surface appeared to have greatest cellular inhabitation (Fig. 4C) along with the higher mean value of pore area filled with skin tissue for the nanotubular surface implants within first three weeks after implantation (Table 4). These results indicate a trend, which might have been significant, given a larger sample size.

Duration of implantation was shown to be a significant factor for the area of skin ingrowth – the longer implant was in contact with skin, the better was skin integration in all 3 types of implants. Thus, our hypothesis 3 was supported.

Skin-implant integration

There is an apparent contradiction between the lower extrusion length (Fig. 5A) and extrusion rate (Table 3) of implants with smaller pores, on the one hand, and the similar amount of skin ingrowth in implants with small and large pores (Figs. 5B and 6), on the other hand. Larger pores would seem to allow easier tissue migration into the deep pores. This trend could be noticed in Fig. 6. It has been postulated that the faster the skin can migrate through the implant (permigration[4]) and regain some type of epidermal continuity, the faster the percutaneous implant will be extruded. This is because increasing pore size increases the strength of skin attachment[40]. Most likely, this was the reason the implants with larger pores were extruded faster in this study. When pore size is smaller, it is more difficult for the tissue to migrate through the pores and thus the implant might be extruded more slowly. These considerations suggest that there may be an optimum pore size that permits sufficient skin ingrowth but does not lead to fast implant extrusions. It is important to note that in this study implants were not anchored to bone; nevertheless, the extrusion length of Small and Nano implants were relatively small (Fig. 5A, Table 3). This could be an indication that pore size 40–100 μm may be close to optimum.

Tissue ingrowth was evident throughout the entire width and length of implant at 3 and 4–6 weeks of implantation, as green-colored area bins (at least 40% of implant pore area filled with tissue) were present in central width bins 4 through 7 (Fig. 6A, B). The maximum skin

ingrowth distance may have been limited in many cases by the reinforcing wires in the central region of implants. Thus, the maximum depth of skin ingrowth was 1.25 mm, i.e. the implant radius (1.5 mm) minus the wire radius (0.25 mm), assuming a wire was placed in the center of the implant. A previous study on skin ingrowth into porous poly(2-hydroxyethyl methacrylate) implants (pore size 40 μm and 60 μm)[11] reported a much lower maximal ingrowth distance of about 90 μm over 3 to 14 days. This difference suggests that skin has better affinity for titanium than for poly(2-hydroxyethyl methacrylate). Implants with porous-coated titanium anchored in bone of sheep for 5 to 9 months have also demonstrated good integration of skin with porous coating[14,24].

While we observed only one case of clinically evident infection out of 35 porous implants (infection rate 2.9%), there is no guarantee that a skin barrier for pathogens was formed inside the implants. Nevertheless, low infection rate in this and other studies[14,24] suggests that skin interface with porous titanium percutaneous implants limits bacterial penetration. Additional studies are needed to confirm these results. It should also be noted that the pores may provide a portal of entry for bacteria into the implant, as bacterial colonies were observed in the exterior pores and serocellular crust (Fig. 4A). Bacteria observed in this study were clusters of cocci morphologically consistent with normal cutaneous flora (i.e. *Staphylococcus spp.)*. Bacterial cultures performed on four implant sites grew *Staphylococcus spp*., consistent with histopathologic observations. Together, these findings suggest that implant infection, if and when it occurs, is likely due to migration of normal skin flora into implant pores.

Presently it is difficult to discern the role of haired skin on skin integration with a porous percutaneous device. Hair may, in the long term, enhance protection of the implants as it provides a loose barrier and has been shown to decrease transdermal drug delivery for some substances[41]. Therefore we presume that it might also reduce the bacterial penetration rate. However, one problem with hair is that the hair shafts get broken off and pushed down into the dermis along with the pylon during the implantation procedure (not shown). The hair shafts then elicit an inflammatory response, which may prevent or delay tissue ingrowth into the device until the inflammation subsides. Thus, the presence of hair may delay skin-implant integration. The presence of hair around the surgical site during the implantation may also prevent proper sterilization and result in a contaminated wound. Therefore a more in-depth study may be needed if animals with extensive body hair will be implanted with percutaneous devices.

Study limitations

There are several limitations of the present study. First, it is unclear what role the bandaging played in the amount of extrusion of the implants. The bandaging was used to prevent self-removal of the implants by the rats; however, it likely reduced the implant extrusion rate. Still, since this type of pylon is designed for attachment of bone-anchored external prostheses[17], no extrusion and thus better skin integration with osseointegrated percutaneous implants can be expected[8,14,24].

The second limitation of the study was a relatively short duration of implantation (3 and 6 weeks). This duration was selected because of the concern that pylons implanted for periods longer than 6 weeks would be extruded and no histological analysis would be possible. This is a limitation typical for studies of percutaneous implants that are not anchored to bone. Despite this limitation we were able to establish the significant effect of implantation time on skin ingrowth.

CONCLUSION

Currently, there are no percutaneous devices for drug delivery, monitoring body internal environment or attaching limb prostheses that permit complete integration of skin with the device and create a long-term skin barrier to prevent pathogens from entering the body. The results of this study demonstrate that percutaneous porous titanium implants with pore sizes of 40–100 μm and 100–160 μm with and without nanotubular surface treatment allow for skin ingrowth of over 50% of total implant porous area over the course of 6 weeks. Longer implantation time (4–6 weeks vs. 3 weeks) resulted in significantly greater skin ingrowth. Although no difference in skin ingrowth area among Small, Large and Nano implants was found, implants with nanotubular surface had more consistent, diffuse fibrovascular ingrowth into the pores of the embedded portion of the device. The results of this study suggest that percutaneous porous titanium implants allow for skin integration with the potential for a safe seal. Future studies of percutaneous porous titanium implants should investigate the extent to which skin ingrowth into implant prevents bacteria from entering the body.

Acknowledgments

We thank Juan Cave II and Ricky Mehta for surgical assistance. The study was supported by NIH training grant to BJF T32-HD055180-02 and the Center for Human Movement Studies at Georgia Tech to BIP. Additional support came from NIH grant R44HD057492 to MP and BIP. We would also like to thank Barbara Smith and Patricia Capellato for their assistance.

8. References

1. von Recum AF, Park JB. Permanent percutaneous devices. Crit Rev Bioeng. 1981; 5(1):37–77. [PubMed: 7014096]
2. Peramo A, Marcelo CL. Bioengineering the skin-implant interface: the use of regenerative therapies in implanted devices. Ann Biomed Eng. 2010; 38(6):2013–31. [PubMed: 20140520]
3. Donlan RM. Biofilms and device-associated infections. Emerg Infect Dis. 2001; 7(2):277–81. [PubMed: 11294723]
4. von Recum AF. Applications and failure modes of percutaneous devices: a review. J Biomed Mater Res. 1984; 18(4):323–36. [PubMed: 6234317]
5. Feldman DS, von Recum aF. Non-epidermally induced failure modes of percutaneous devices. Biomaterials. 1985; 6:352–6. [PubMed: 4052549]
6. Schreuders PD, Salthouse TN, von Recum aF. Normal wound healing compared to healing within porous Dacron implants. J Biomed Mater Res. 1988; 22:121–35. [PubMed: 2451676]
7. Krouskop TA, Brown HD, Gray K, Romovacek GR, Spira M, Runyan RS. Bacterial challenge study of a porous carbon percutaneous implant. Biomaterials. 1988; 9:398–404. [PubMed: 3146992]
8. Jansen, Ja; van der Waerden, JP.; van der Lubbe, HB.; de Groot, K. Tissue response to percutaneous implants in rabbits. J Biomed Mater Res. 1990; 24:295–307. [PubMed: 2318897]
9. Fukano Y, Usui ML, Underwood RA, Isenhath S, Marshall aJ, Hauch KD, Ratner BD, Olerud JE, Fleckman P. Epidermal and dermal integration into sphere-templated porous poly(2-hydroxyethyl methacrylate) implants in mice. J Biomed Mater Res A. 2010; 94:1172–86. [PubMed: 20694984]
10. Knowles NG, Miyashita Y, Usui ML, Marshall AJ, Pirrone A, Hauch KD, Ratner BD, Underwood Ra, Fleckman P, Olerud JE. A model for studying epithelial attachment and morphology at the interface between skin and percutaneous devices. Journal of biomedical materials research. Part A. 2005; 74:482–8. [PubMed: 15983994]
11. Underwood RA, Usui ML, Zhao G, Hauch KD, Takeno MM, Ratner BD, Marshall AJ, Shi X, Olerud JE, Fleckman P. Quantifying the effect of pore size and surface treatment on epidermal incorporation into percutaneously implanted sphere-templated porous biomaterials in mice. J Biomed Mater Res A. 2011; 98:499–508. [PubMed: 21681942]

12. Stynes G, Kiroff GK, Morrison WaJ, Kirkland Ma. Tissue compatibility of biomaterials: benefits and problems of skin biointegration. ANZ J Surg. 2008; 78:654–9. [PubMed: 18796021]
13. Chou TG, Petti CA, Szakacs J, Bloebaum RD. Evaluating antimicrobials and implant materials for infection prevention around transcutaneous osseointegrated implants in a rabbit model. J Biomed Mater Res A. 2010; 92:942–52. [PubMed: 19291687]
14. Perry EL, Beck JP, Williams DL, Bloebaum RD. Assessing peri-Implant tissue infection prevention in a percutaneous model. J Biomed Mater Res B Appl Biomater. 2009:397–408.
15. Pitkin M, Raykhtsaum G, Galibin OV, Protasov MV, Chihovskaya JV, Belyaeva IG. Skin and bone integrated prosthetic pylon: A pilot animal study. J Rehabil Res Dev. 2006; 43:573. [PubMed: 17123195]
16. Pitkin M, Raykhtsaum G, Pilling J, Galibin OV, Protasov MV, Chihovskaya JV, Belyaeva IG, Blinova MI, Yudintseva NM, Potokin I, et al. Porous composite prosthetic pylon for integration with skin and bone. J Rehabil Res Dev. 2007; 44:723–738. [PubMed: 17943684]
17. Pitkin M, Raykhtsaum G, Pilling J, Shukeylo Y, Moxson V, Duz V, Lewandowski J, Connolly R, Kistenberg RS, Dalton JF IV, et al. Mathematical modeling and Mechanical and histopathological testing of porous prosthetic pylon for direct skeletal attachment. J Rehabil Res Dev. 2009; 46:315–330. [PubMed: 19675985]
18. Pitkin M, Pilling J, Raykhtsaum G. Mechanical properties of totally permeable titanium composite pylon for direct skeletal attachment. J Biomed Mater Res B Appl Biomater. 2012; 100(4):993–9. [PubMed: 22287509]
19. Davis SD, Gibbons DF, Martin RL, Levitt SR, Smith J, Harrington RV. Biocompatibility of ceramic implants in soft tissue. J Biomed Mater Res. 1972; 6:425–49. [PubMed: 4342035]
20. Jansen JA, Paquay YG, van der Waerden JP. Tissue reaction to soft-tissue anchored percutaneous implants in rabbits. J Biomed Mater Res. 1994; 28(9):1047–54. [PubMed: 7814432]
21. Tjellstrom A, Lindstrom J, Nylen O, Albrektsson T, Branemark PI. Directly bone-anchored implants for fixation of aural epistheses. Biomaterials. 1983; 4(1):55–7. [PubMed: 6838958]
22. Tjellstrom A, Lindstrom J, Hallen O, Albrektsson T, Branemark PI. Direct bone anchorage of external hearing aids. J Biomed Eng. 1983; 5(1):59–63. [PubMed: 6827820]
23. Hagberg K, Branemark R. One hundred patients treated with osseointegrated transfemoral amputation prostheses--rehabilitation perspective. J Rehabil Res Dev. 2009; 46(3):331–44. [PubMed: 19675986]
24. Jeyapalina S, Beck JP, Bachus KN, Williams DL, Bloebaum RD. Efficacy of a porous-structured titanium subdermal barrier for preventing infection in percutaneous osseointegrated prostheses. J Orthop Res. 2012; 30(8):1304–11. [PubMed: 22294380]
25. Snik AFM, Mylanus EaM, Proops DW, Wolfaardt JF, Hodgetts WE, Somers T, Niparko JK, Wazen JJ, Sterkers O, Cremers CWRJ, et al. Consensus statements on the BAHA system: where do we stand at present? Ann Otol Rhinol Laryngol Suppl. 2005; 195:2–12. [PubMed: 16619473]
26. Branemark PI. Osseointegration and its experimental background. J Prosthet Dent. 1983; 50:399–410. [PubMed: 6352924]
27. Bonding P. Titanium implants for bone-anchored hearing aids--host reaction. Acta Otolaryngol Suppl. 2000; 543:105–7. [PubMed: 10908993]
28. Branemark PI, Albrektsson T. Titanium implants permanently penetrating human skin. Scand J Plast Reconstr Surg. 1982; 16(1):17–21. [PubMed: 7112035]
29. Pitkin M. Design features of the implants for direct skeletal attachment of limb prostheses. J Biomed Mater Res A. 2013 in press.
30. Isackson D, McGill LD, Bachus KN. Percutaneous implants with porous titanium dermal barriers: an in vivo evaluation of infection risk. Med Eng Phys. 2011; 33(4):418–26. [PubMed: 21145778]
31. Winter GD. Transcutaneous implants: reactions of the skin-implant interface. J Biomed Mater Res. 1974; 8:99–113. [PubMed: 4616966]
32. Puckett SD, Lee PP, Ciombor DM, Aaron RK, Webster TJ. Nanotextured titanium surfaces for enhancing skin growth on transcutaneous osseointegrated devices. Acta Biomater. 2010; 6:2352–62. [PubMed: 20005310]

33. Chehroudi B, Brunette DM. Subcutaneous microfabricated surfaces inhibit epithelial recession and promote long-term survival of percutaneous implants. Biomaterials. 2002; 23(1):229–37. [PubMed: 11762842]
34. Tang X, Li D. Fabrication, geometry, and mechanical properties of highly ordered TiO_2 nanotubular arrays. J Phys Chem. 2009; 113(17):7107–7113.
35. Farrell, BJ.; Pitkin, M.; Popat, K.; Prilutsky, BI. Effect of pore size, implantation time and nano-surface properties on rat skin ingrowth into porous titanium. San Francisco, CA: Feb 10. 2012
36. Pitkin, M.; Raykhtsaum, G. Skin integrated device. US patent 8257435. 2012.
37. Ruckh T, Porter JR, Allam NK, Feng X, Grimes CA, Popat KC. Nanostructured tantala as a template for enhanced osseointegration. Nanotechnology. 2009; 20(4):045102. [PubMed: 19417310]
38. Schneider CA, Rasband WS, Eliceiri KW. NIH Image to ImageJ: 25 years of image analysis. Nat Methods. 2012; 9(7):671–675. [PubMed: 22930834]
39. Torralba KD, Quismorio FP Jr. Soft tissue infections. Rheum Dis Clin North Am. 2009; 35(1):45–62. [PubMed: 19480996]
40. Bobyn JD, Wilson GJ, MacGregor DC, Pilliar RM, Weatherly GC. Effect of pore size on the peel strength of attachment of fibrous tissue to porous-surfaced implants. J Biomed Mater Res. 1982; 16:571–84. [PubMed: 7130213]
41. Lauer AC, Elder JT, Weiner ND. Evaluation of the hairless rat as a model for in vivo percutaneous absorption. J Pharm Sci. 1997; 86(1):13–8. [PubMed: 9002453]

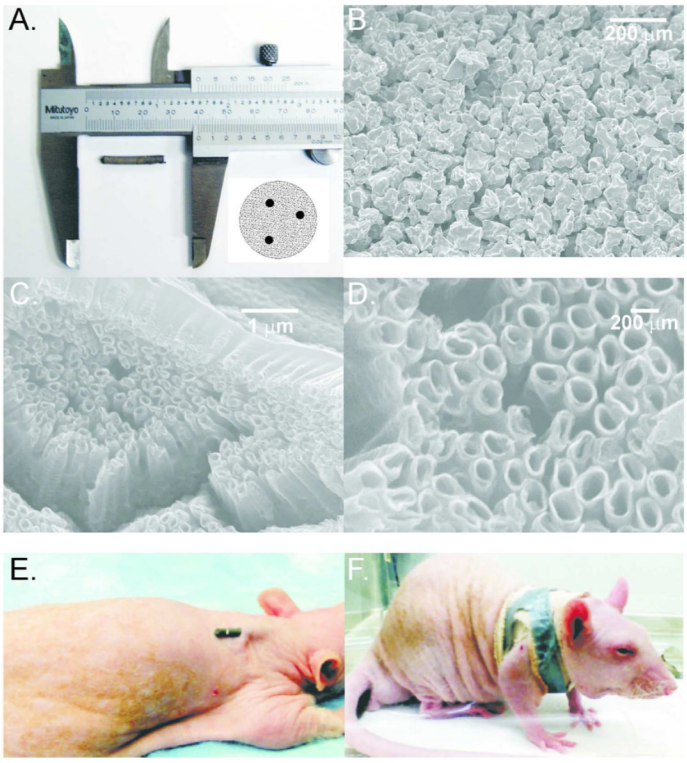

Figure 1.
Implants and implantation method. A: An example of implant used in experiments; the insert shows a diagram of an implant cross-section with 3 thin titanium reinforcing wires. B: Scanning electron micrograph (SEM) of small pore implant without nanotube addition (100x magnification). C: SEM of small pore implant with nanotube addition (20,000x magnification). D: Detailed SEM of nanotube surface structures (50,000x magnification). E: and F: Illustration of implant location and orientation in the back of an anesthetized rat and how implant was secured.

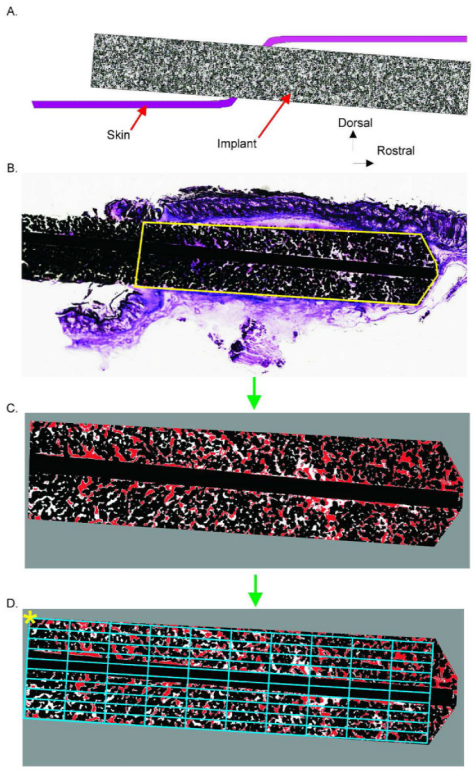

Figure 2.

Implant image analysis steps. A: Cartoon illustrating a longitudinal cross-section through the skin and implant. B–D: Image processing steps. B: Implant outline identified for histomorphometry. C: Resulting image after thresholding. D: Area bin definition for binned implant area. Asterisk indicates corner of $bin_{1,1}$

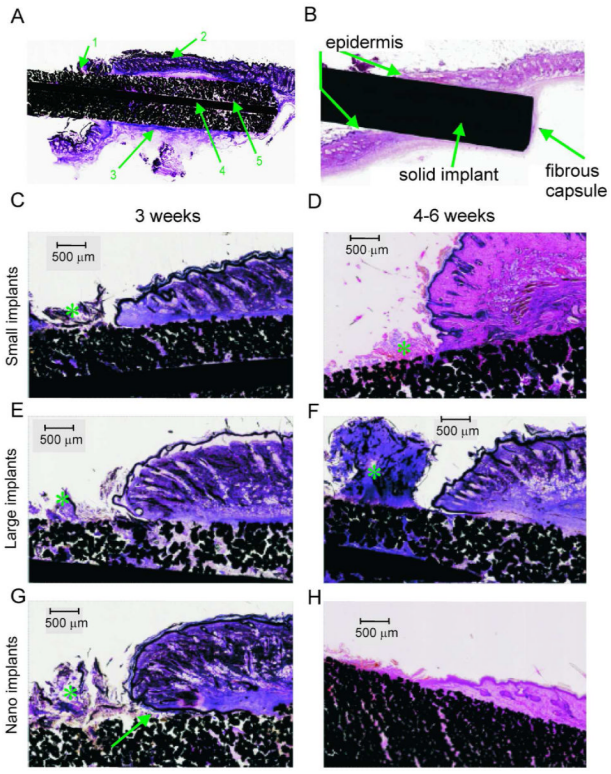

Figure 3.

Representative stained (haematoxylin and basic fuchsin) sections of implants with small pore size (Small), large pore size (Large) and small pore size with nano-surface treatment (Nano) at 3 and 6 weeks after implantation. Top panels: Typical tissue features in stained sections through a porous (A) and solid (B) implants. 1: Serocellular crust on exterior side of implant. 2: Skin on upper edge of implant. 3: Fibrous capsule surrounding implant. 4: Central reinforcing wire. 5: Deep skin ingrowth into pores of implant. C–H: Examples of tissue ingrowth into 3 implant types and across different implantation durations (all magnifications are 2x). Asterisk (*) indicates serocellular crust. Arrow in G shows a pocket with cellular debris at the epidermal-implant interface.

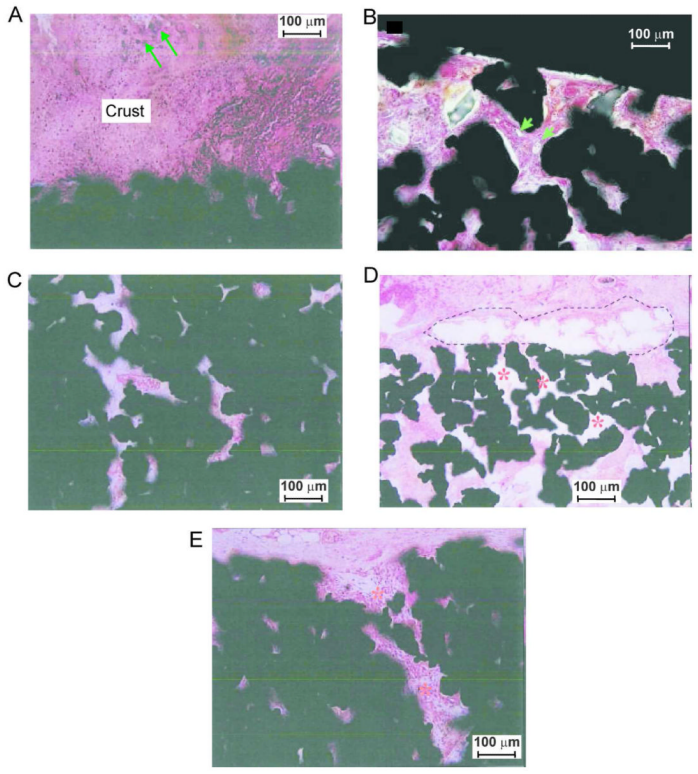

Figure 4.

Illustrations of fibrovascular ingrowth into porous implants. Implant sections are stained with haematoxylin and basic fuchsin. A: Bacterial colonization (arrows) of the surface crust; bacteria were not identified in the pores of the implant (Nano implant, 6 weeks, SD rat, magnification 200x). B: Small vessels (arrows) in fibrous tissue inside implant pores (Large implant, 4 weeks, CD rat, magnification 200x). C: The innermost pores of the device show diffuse fibrovascular ingrowth without significant inflammation (Nano implant, 6 weeks, SD rat, magnification 200x). D: Poor tissue ingrowth (*) into pores of the implant adjacent to a focus of granulomatous inflammation (dashed lines) (Small implant, 6 weeks, SD rat, magnification 40x). E: Mononuclear infiltrates (*) extending into the pores of the periphery of the implant (Nano implant, 6 weeks, SD rat, magnification 200×).

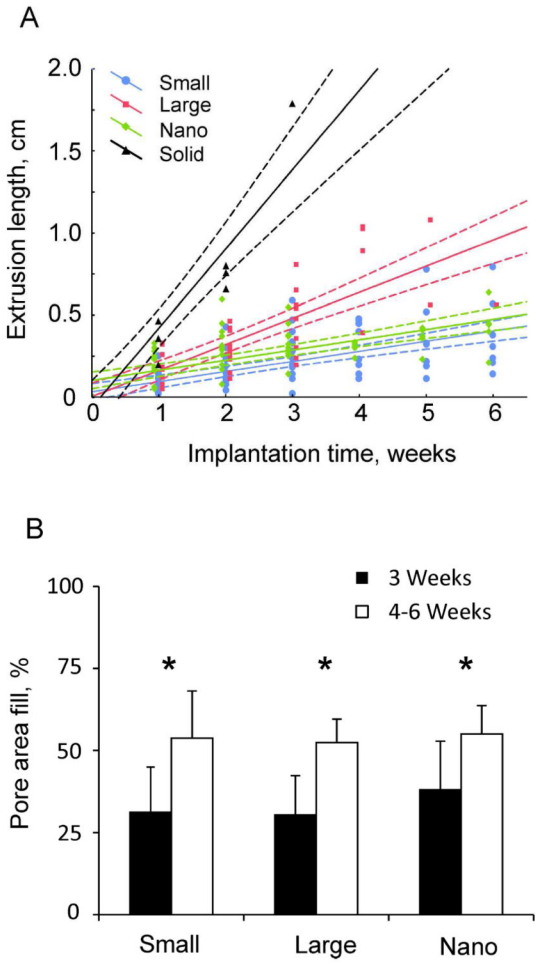

Figure 5.

A: Extrusion length for each implant type as a function of implantation time; solid lines are linear regression lines, dashed lines are 95%-confidence limits. Linear regression equations between implantation time (x, weeks) and extrusion length (y, cm) are as follows. Solid implants: $y=-0.0642+0.4833*x$ ($r=0.946$, $p<0.05$); Large implants: $y=0.002+0.1591*x$ ($r=0.824$, $p<0.05$); Small implants: $y=0.0315+0.0619*x$ ($r=0.657$, $p<0.05$); Nano implants: $y=0.1008+0.0621*x$ ($r=0.704$, $p<0.05$).

B: Percentage of total pore area filled with stained tissue (mean+SD). The data from pylons that remained implanted beyond 4 weeks (see Table 2) were combined into the 4–6 week implantation group for purposes of statistical analysis. * indicates significant ($p < 0.05$) difference between 3 weeks and 4–6 weeks of implantation. No differences were found between implant types.

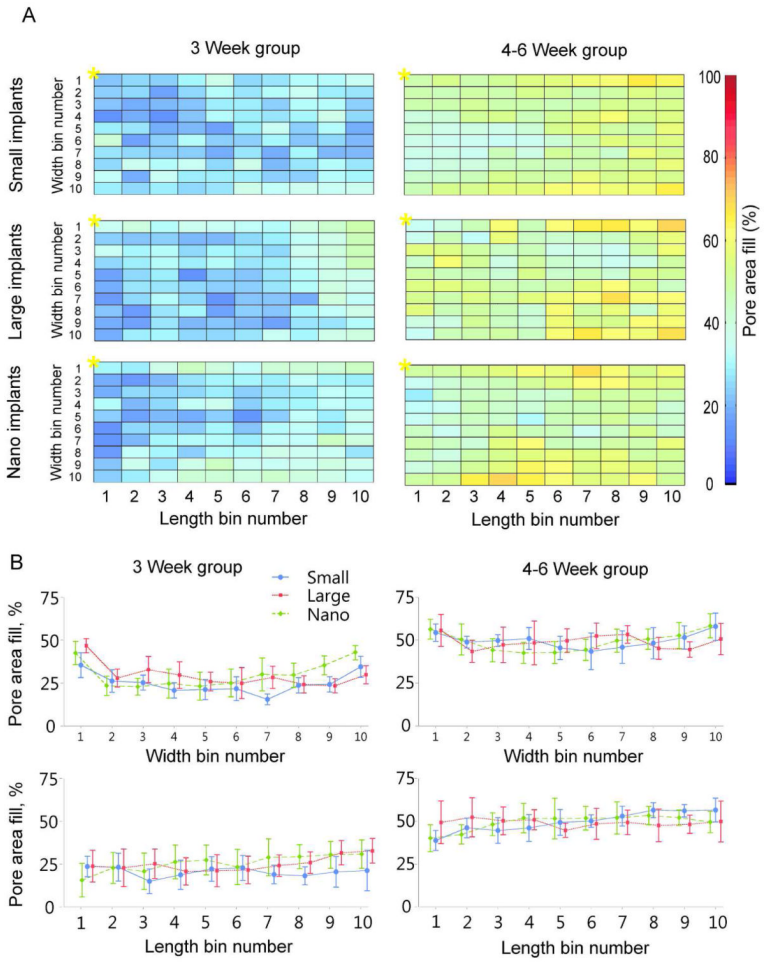

Figure 6.

Distribution of mean skin ingrowth within different porous implants. A: Each panel represents normalized pore area of implant under the skin. The area is divided into 100 bins. The top row of bins in each panel indicates the pore area at the upper edge of implant right under the dermis. The left most column represents the bins that would line along the implant exit site; * indicates bin1,1 (see Fig. 2 D for further details). Percentage pore area filed with skin tissue is shown for each bin by color. B (top panels): Skin ingrowth (±SD) averaged across length bins as a function of implant width for each type of implant and implantation period – 3 weeks (left panels) and 4–6 weeks (right panels). Bottom panels: Skin ingrowth (±SD) averaged across width bins as a function of implant length for each type of implant and implantation period.

Table 1

Study design and experimental groups. Solid group designates animals implanted with solid pylons; Small group, animals implanted with pylons of small pore size 40–100 μm; Large group, animals with pylons of larger pore size 100 – 160 μm; Nano group had implanted pylons with pore size 40–100 μm and a nanotubular surface treatment.

Groups	Rat type	3 Weeks	6 Weeks	Total
Solid	SD	5		5
Small	Hairless	5	5	10
Small	SD		5	5
Large	Hairless	5	5	10
Nano	Hairless	5		5
Nano	SD		5	5

Table 2

Total number of implants remaining in the skin through each week of the study. Note that 5 Small, 5 Large and 5 Nano implant types were harvested from rats who reached the 3-week time endpoint. The number of implanted rats is shown in Table 1.

Implant type	1 Week	2 Weeks	3 Weeks	4 Weeks	5 Weeks	6 Weeks
Solid	3	3	1			
Small	15	15	15	10	9	9
Large	10	10	10	5	2	1
Nano	10	10	10	5	5	5

Table 3

Slope of linear regression (mean extrusion rate) for each group of implanted animals (in cm/week, see Fig. 5A).

Implant type	Slope of linear regression (±95%-confidence limits)
Solid	$0.483 \pm 0.166^{\dagger *}$
Large	$0.159 \pm 0.033^{\dagger \ddagger}$
Small	$0.062 \pm 0.016^{\dagger}$
Nano	$0.062 \pm 0.017^{\dagger}$

†Significantly different from zero;

*Significant difference between Solid and other implant groups ($p < 0.05$);

‡Significant difference between Large and other implant groups ($p < 0.05$).

Table 4

Mean percentage of implant area filled with skin tissue for three different porous implants three weeks after implantation

Implant type	Percent (%) of implant area filled (mean±SD)
Small	31.2± 13.7
Large	30.4±11.9
Nano	38.0±14.8